Seismic Imaging of the Far Side and Interior of the Sun

D. C. Braun

NorthWest Research Associates, Colorado Research Associates Division

C. Lindsey

Solar Physics Research Corporation

SUMMARY

Images of active regions on the far side of the Sun were derived by applying seismic holography to observations from the SOI-MDI (Solar Oscillations Investigation – Michelson Doppler Imager) instrument on the *SOHO* spacecraft. Synoptic seismic imaging of far-side solar activity will allow anticipation of the appearance of large active regions more than a week ahead of their arrival on the east limb. The technical requirements for a synoptic monitor appear to be quite modest, given real time access to observations from MDI or the Global Oscillations Network Group.

In addition to providing new applications for space weather prediction, the development of solar acoustic holography is opening major new diagnostic avenues in the study of the solar interior. Phase-sensitive seismic holography is producing high-resolution maps of sound travel-time anomalies caused by magnetic forces in the immediate subphotosphere, apparent thermal enhancements in acoustic moats around sunspots, and Doppler signatures of subsurface flows. Seismic holography applied to global modes, such as those used to image the far side, has directly demonstrated the influence of active regions on these modes. This reinforces a growing consensus that reduced sound travel times in magnetic regions explain the entirety of the frequency shifts of global modes with the solar cycle. Phase-sensitive holography will also be used to probe thermal and Doppler perturbations deep in the solar convection zone and the tachocline.

HELIOSEISMIC HOLOGRAPHY was proposed a decade ago (Lindsey & Braun 1990) and developed conceptually by Braun et al. (1992) and Lindsey & Braun (1997, 2000b) as a general diagnostic basis for local helioseismology, with the purpose of imaging of local acoustic anomalies in the solar interior and on the far side.

The principle of *far-side* seismic holography is illustrated in this cross-section of the solar interior. Wavefronts emanating from a far-side point source (focal point) at intervals of 286 sec (1/3.5 mHz) within the corridor of trajectories shown reflect once from the solar surface (right and left sides) and arrive in an annular pupil on the near surface (bottom) of the sun. Waves coherently emanating from the focal point (green arrows) are represented by the acoustic egression (H_+), reconstructed for each focal point in the image from the surface disturbance it creates on the near surface. Its time reverse signature, the ingression (H_-, yellow arrows), represents identical waves coherently converging into the focal point to contribute to the local disturbance there. A local acoustic depression at the focal point will produce a reduction in the acoustic travel-time, and shift the phase of the ingression-egression correlation. In the case of a quasi-specular reflection at the focal point, the outside of the ingression pupil on one side (red part of wavefronts) correlates with the outside of the ingression pupil on the other (also red). Likewise for the inside of the pupil (blue part of wavefronts). Thus, the loss of either side of the pupil destroys the phase correlation for the entire pupil. For this reason, phase-sensitive holography of far-side solar activity is only practical for regions within approximately 50° of the antipode of disk center. The dotted circle indicates the depth of the base of the solar convection zone.

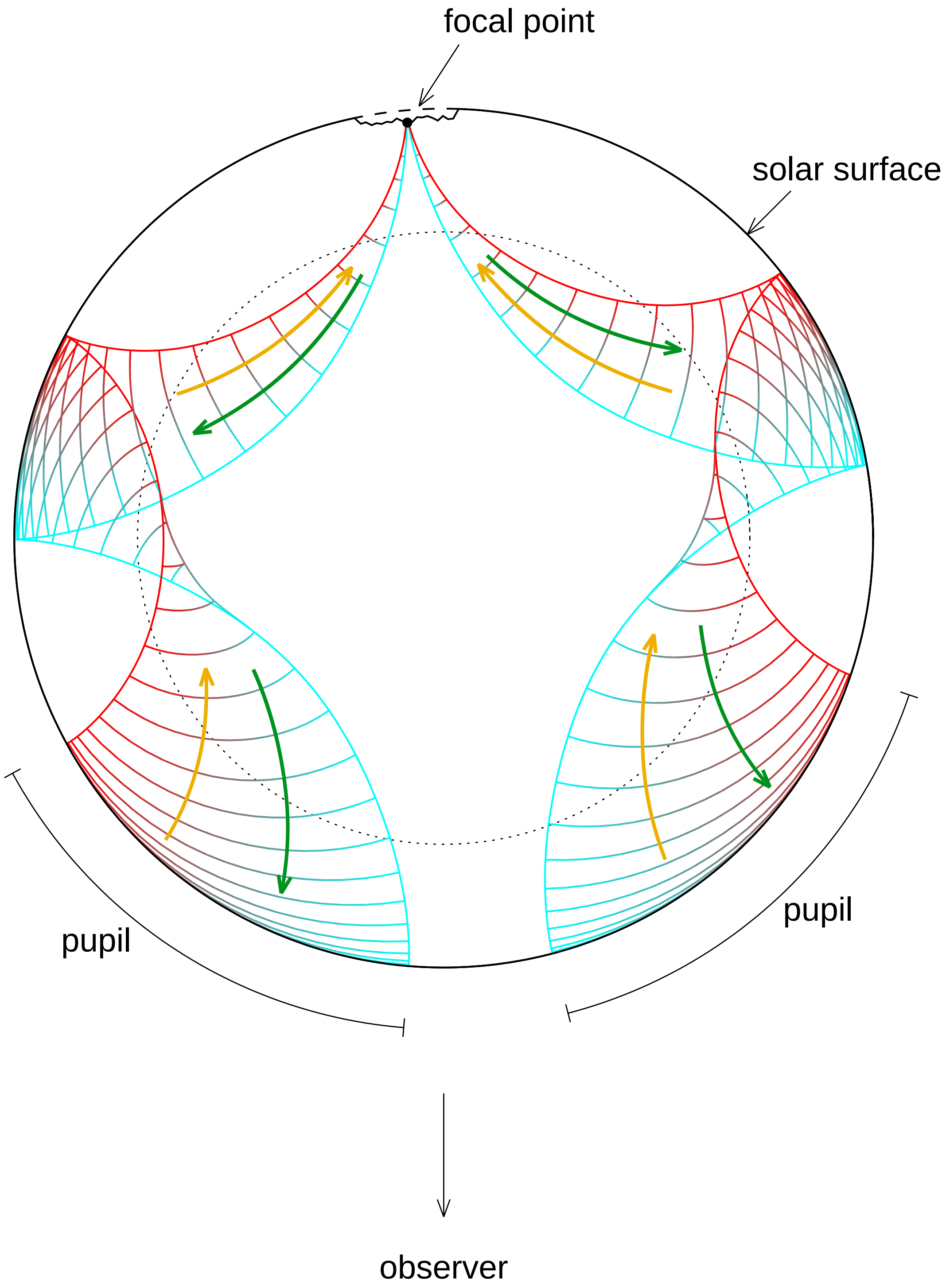
focal point
solar surface
pupil
pupil
observer

SEISMIC HOLOGRAPHY OF THE NEAR SOLAR INTERIOR is illustrated for a complex active region, NOAA AR 8179, for which an MDI magnetogram is shown in panel **a**. Standard acoustic power holography is accomplished by mapping the egression power, $|H_+|^2$, which is here integrated for a 24 hr period and over a 1-mHz frequency band centered at 3 mHz (panel **b**). This diagnostic is sensitive to acoustic sources and absorbers, the latter of which are rendered as silhouettes.

In addition, phase-sensitive holography (Lindsey & Braun 1997) is used to gauge acoustic travel-time perturbations, Δt, caused by refractive anomalies or the magnetic depressions of sunspots and plages (Braun 1995; Duvall, et al. 1996; Braun & Lindsey 2000). Panel **c** shows a map of Δt at 5 mHz determined from the phase of the egression-ingression correlation. Panel **d** compares the mean 3 mHz travel-time perturbation for an isolated plage (enclosed by the dashed line in panel **a**) with that of plages in the "acoustic moat" (the area between the regions enclosed by the dotted and solid lines). The additional time delay in the moats may be explained by a thermal excess in the moat subphotosphere due to the blockage of convective transport by the overlying sunspot photosphere.

Braun & Lindsey (2000) present statistics to suggest that the entirety of the frequency shifts of global modes with the solar cycle can be explained by the superficial phase shifts due to plages, acoustic moats, and sunspots, in that order of estimated importance. This is consistent with recent work by Howe, et al. (1999) and Hindman, et al. (2000), and similar work by Cunha, et al. (1998), who consider only sunspots.

All of the seismic images shown here were derived from helioseismic observations made with the SOI-MDI instrument on *SOHO*, which is described by Scherrer, et al. (1995).

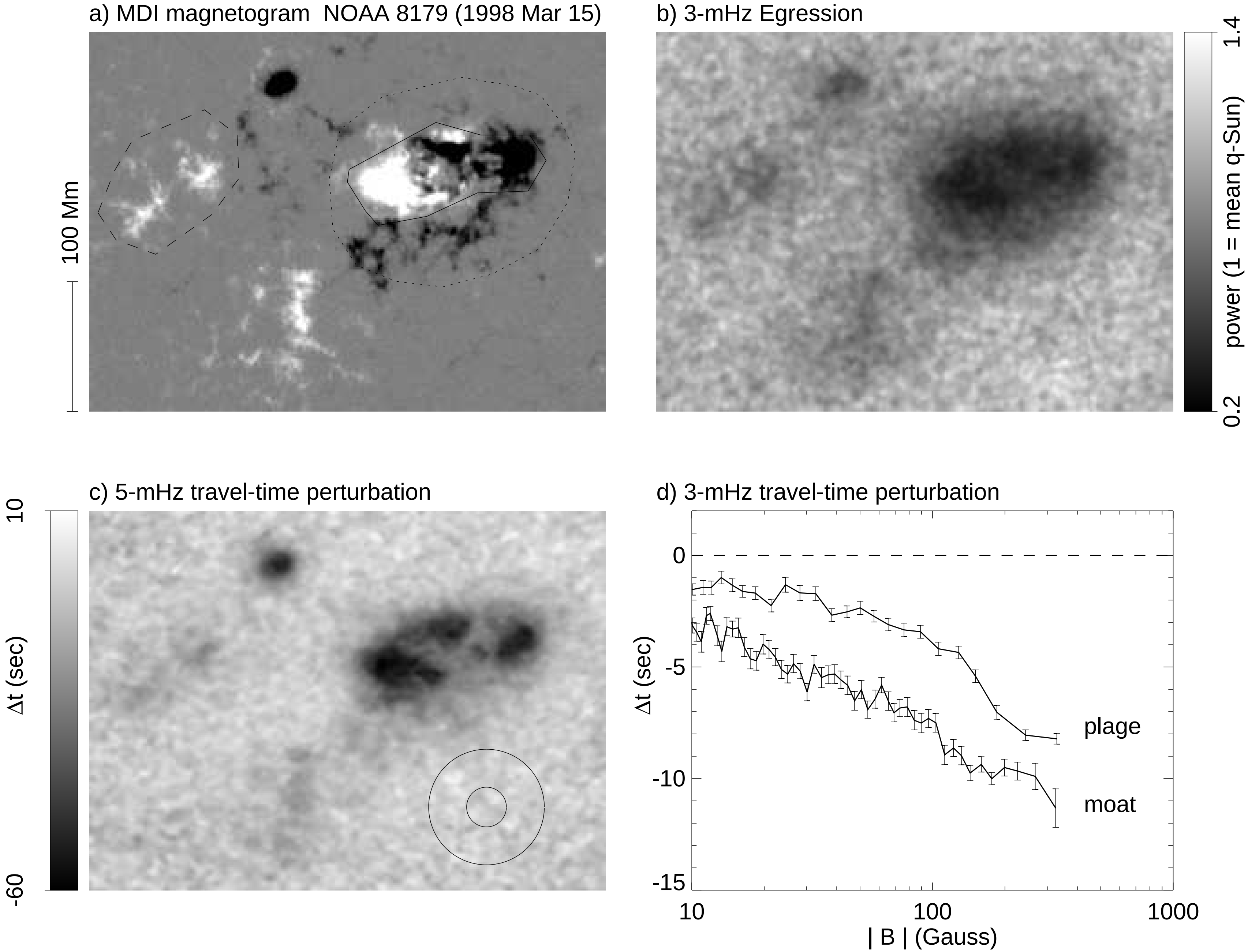
a) MDI magnetogram NOAA 8179 (1998 Mar 15)
100 Mm
b) 3-mHz Egression
power (1 = mean q-Sun)
1.4
0.2
c) 5-mHz travel-time perturbation
Δt (sec)
10
-60
d) 3-mHz travel-time perturbation
Δt (sec)
0
-5
-10
-15
plage
moat
10
100
1000
| B | (Gauss)

THE FIRST IMAGES OF THE FAR SIDE OF THE SUN from Lindsey & Braun (2000a). The top two frames show maps of the sound travel-time pertubation Δt, referenced to the mean quiet-Sun value (Δt=0), in the neighborhood of NOAA AR 8194 just before (**A**) and during (**B**) its passage through the far-side solar meridian. (**C**) a magnetogram of the same location a week and a half later, as the active region becomes visible just inside of the east limb. To derive these images, we computed two-skip egression and ingression maps over the spectral range 2.5–4.5 mHz using a near-side pupil illustrated earlier. At 3.5 mHz, this pupil samples waves with ℓ predominantly in the range 22–40. This imposes a diffraction limit of $\sim$10° of longitude at the solar equator, easily resolving a moderately large plage. The active region is indicated by a local reduction ($\Delta t < 0$) in the sound travel-time of about 6 s over an area covering about 300 degree^2. This is consistent with the sign and magnitude of signatures that typically characterize plages imaged on the near side of the Sun. All three maps are overhead-view Postel projections centered on the Carrington coordinates $L = 29.78°$, $B = -22.82°$ (marked by fiducials) with radial distance from the above reference point indicated by the rule just beneath the bottom frame.

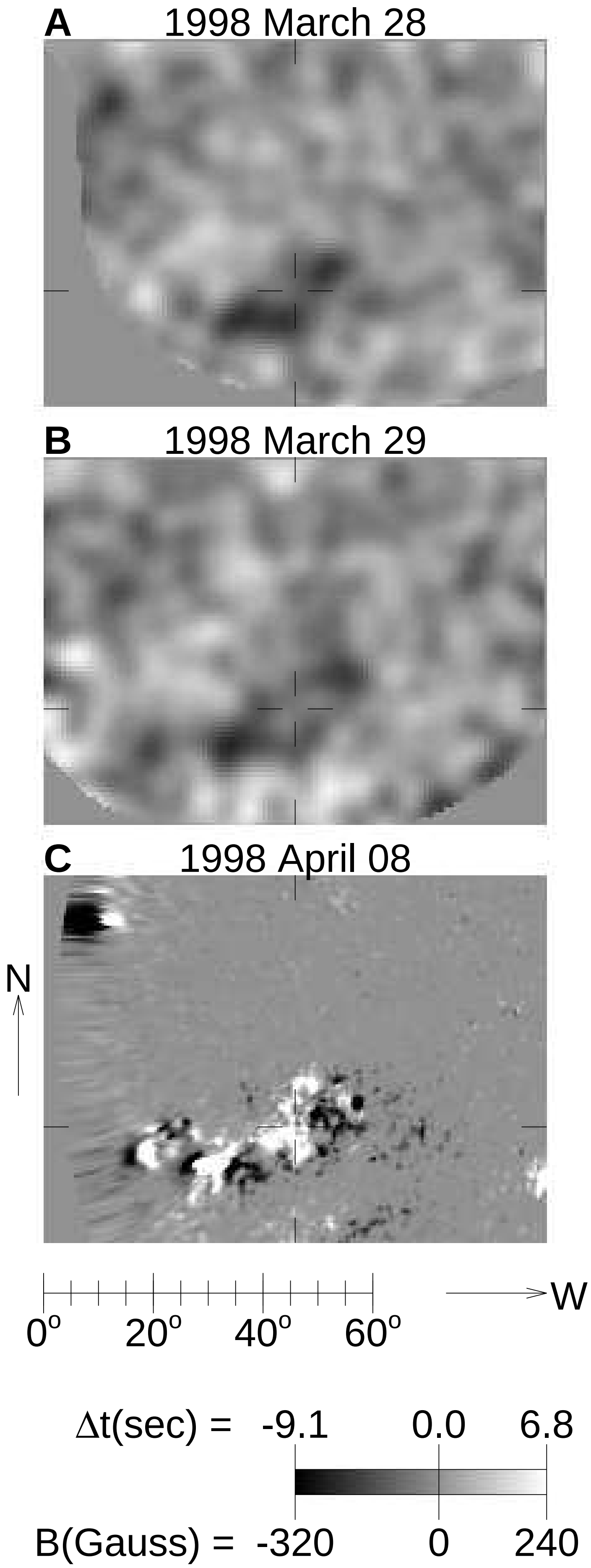
A
1998 March 28
B
1998 March 29
C
1998 April 08
N
W
0°
20°
40°
60°
Δt(sec) = -9.1 0.0 6.8
B(Gauss) = -320 0 240

COMPARATIVE TRAVEL-TIME MAPS OF THE NEAR AND FAR SIDE of the Sun show that far-side images are not substantially contaminated by near-side artifacts. A magnetogram on 28 March 1998 (panel **a**) is compared with seismic images focused on the near side of the Sun (panel **b**) and the far side (panel **c**) on the same day. The near-side images (**a** and **b**) are flipped about the horizontal axis through disk center, so that Carrington north is towards the bottom of the page. This way, each pixel in either near-side image matches the location of its antipode in the far-side image (**c**). Fiducials mark the position of a sunspot in NOAA AR 8185 in panels **a** and **b** and its antipode in **c**. Near-side seismic images sometimes show significant features that do not appear in magnetograms, which may be signatures of near-side but subsurface acoustic anomalies. However, the lack of any significant far-side signature at the antipode of AR 8185 shows that artifacts in far-side images due to near-side features are not apparent. In general, we have never encountered such artifacts or found any compelling reasons to expect them.

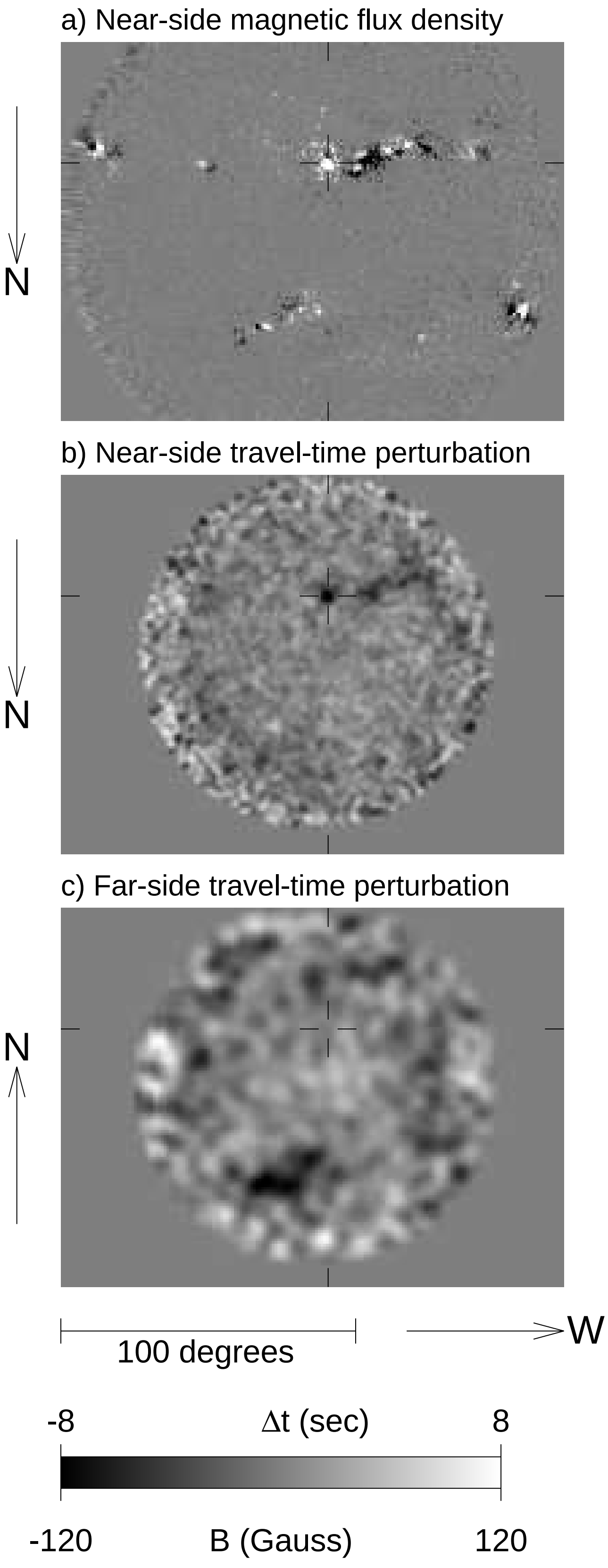
a) Near-side magnetic flux density
N
b) Near-side travel-time perturbation
N
c) Far-side travel-time perturbation
N
100 degrees
W
-8
Δt (sec)
8
-120
B (Gauss)
120

MONITORING ACTIVE REGIONS ON THE SOLAR FAR-SIDE would greatly improve forecasts of of space weather. This figure illustrates a series of seismic images of the far side of the Sun over a ten day period, derived from SOI-MDI observations. Each day is represented by a pair of images: the upper frame shows a travel-time map of the solar far side, integrated over a 24 hour period, while the bottom frame shows a magnetogram of the same region after it has rotated to the near side two weeks later. The images show seismic signatures of several active regions, including one, marked by arrows, which is clearly visible on the far side for seven consecutive days.

Synoptic seismic imaging of far-side solar activity will allow anticipation of the appearance of large active regions more than a week ahead of their arrival on the east limb. The technical requirements for a synoptic monitor appear to be quite modest, given real time access to observations from MDI or the Global Oscillations Network Group, for example. Currently, seismic images of the solar far side are easily computed in just a few hours using a single-processor Pentium-based PC running Linux.

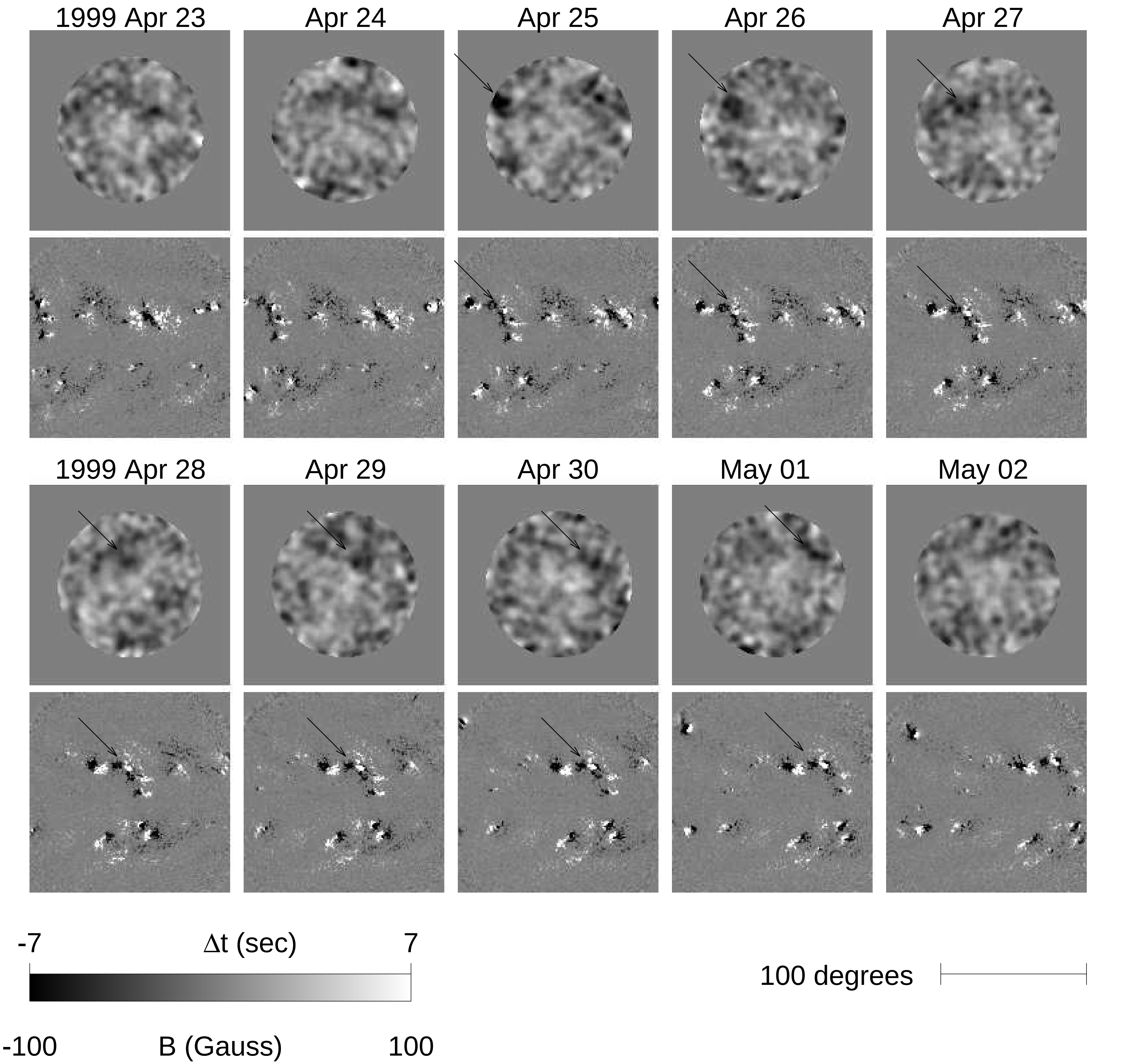

1999 Apr 23
Apr 24
Apr 25
Apr 26
Apr 27
1999 Apr 28
Apr 29
Apr 30
May 01
May 02
-7
Δt (sec)
7
100 degrees
-100
B (Gauss)
100

ACKNOWLEDGMENTS AND REFERENCES

We greatly appreciate the support we have gotten from Dr. P. Scherrer, an early and enthusiastic proponent of far-side imaging, and of the *SOHO* SOI-MDI team. DCB, jointly affiliated with SPRC and NWRA-CoRA, was financially supported through SPRC for this work. *SOHO* is a project of international cooperation between ESA and NASA. This research has been supported by grants from the Stellar Astronomy & Astrophysics and the Solar–Terrestrial programs of the National Science Foundation, the National Aeronautics and Space Administration, and Stanford University.

Braun, D. C. 1995, *ApJ*, **451**, 859.

Braun, D. C. & Lindsey, C. 2000, *Solar Phys.*, **192**, 305.

Braun, D. C., Lindsey, C., Fan, Y., & Jefferies, S. M. 1992, *ApJ*, **392**, 739.

Cunha, M., Brüggen, M., & Gough, D. O. 1998, in S. G. Korzennik and A. Wilson (eds.), *Structure and Dynamics of the Interior of the Sun and Sun-like Stars*, ESA, SP-418, p. 905.

Duvall, T. L. Jr., D'Silva, S., Jefferies, S. M., Harvey, J. W., & Schou, J. 1996, *Nature*, **379**, 235.

Hindman, B. W., Haber, D. A., Toomre, J., & Bogart, R. 2000, *Solar Phys.*, **192**, 361.

Howe, R., Komm, R., & Hill, F. 1999, *ApJ*, **524**, 1084.

Lindsey, C. & Braun, D. C. 1990, *Solar Phys.*, **126**, 101.

Lindsey, C. & Braun, D. C. 1997, *ApJ*, **485**, 895.

Lindsey, C. & Braun, D. C. 2000a, *Science*, **287**, 1799.

Lindsey, C. & Braun, D. C. 2000b, *Solar Phys.*, **192**, 259.

Scherrer, P. H. et al. 1995, *Solar Phys*, **162**, 129.

Copies of this poster, and reprints of related publications, may be obtained at
`http://www.colorado-research.com/~dbraun`